2024 IEEE International Conference on Robotics and Automation (ICRA 2024)
May 13-17, 2024. Yokohama, Japan

Automated Surgical Knot Tying on Mini-Incision with Micro-Suture based on Dual-Arm Nanorobot under Stereo Microscope

Yujie Jiang, Xiang Fu, Chengxi Zhong, Teng Li, Haojian Lu, and Song Liu, *Member, IEEE*

***Abstract*—Knot tying is an essential task for robotic surgery, which is routinely realized by dual-arm robotic manipulation. Despite the well-established protocol and progress at macro scale so far, there remain challenges to further advance robotic knot tying technique, particularly in terms of decreasing space consumption with better dexterity, higher precision, and well biomechanical compatibility. In this paper, we propose a novel dual-arm nanorobotic system setup for automated knot tying performed on mini-incision under stereo microscope, featured by an additional rotation degree of freedom mounted on each arm. With this setup, an optimized motion trajectory planning under standard knot-tying protocol is also presented in order to support tying knots with shorter and thinner suture. Leveraging the natural advantage of nanorobotics and microscope, the proposed system is capable of tying consecutive throws with micro-suture on mini-incision, like in vascular anastomosis or microsurgery. We successfully evaluated the knot tying system on 2.0 mm wide bionic blood vessel with 30 mm long #8-0 micro-suture. We finally tested the mechanical strength of the knots for potential medical assessment.**

I. Introduction

Knot tying is ubiquitous in clinical surgery [1-3], while knot quality is crucial to surgery success and postoperative recovery [4]. In clinical practice, knot tying is generally operated by skilled surgeons manually. Consequently, the quality consistency of surgical knots is not always guaranteed, leading to risk of surgery complex or infection [5]. In this regard, researchers put extensive efforts on automated robot systems to perform this intricate task [6]. Compared to manual operations, automated robot systems are highly procedural with better execution stability, repeatability and dexterity, providing controllable quality for surgery [7]. Thus, the investigation of knot tying by virtue of automated robot systems is significantly attractive and promising. Despite the notable progress so far, challenges persist in advancing robotic knot tying techniques, particularly in terms of minimizing spatial constraints, enhancing dexterity, elevating precision, and ensuring robust biomechanical compatibility.

*This work was supported in part by National Natural Science Foundation of China under Grand 62303321 and Shanghai Pujiang Talents Program under grant 21PJ1410500. (Y. Jiang and X. Fu contribute equally to this work.) (Corresponding author: *Haojian Lu and Song Liu*).

Y. Jiang, X. Fu, C. Zhong, and T. Li are with the School of Information Science and Technology, ShanghaiTech University, Shanghai, China (Email: jiangyj12023@shanghaitech.edu.cn, fuxiang@shanghaitech.edu.cn, zhongchx@shanghaitech.edu.cn, liteng1@shanghaitech.edu.cn).

H. Lu is with the College of Control Science and Engineering, Zhejiang University, Hangzhou, China (Email: luhaojian@zju.edu.cn).

S. Liu is with the School of Information Science and Technology, ShanghaiTech University, Shanghai, China, and with Shanghai Engineering Research Center of Intelligent Vision and Imaging, Shanghai, China (e-mail: liusong@shanghaitech.edu.cn).

There have been extensive efforts from literature towards automated surgical knot tying in robotics field [8-17]. From the perspective of robot system setup, four-arm based [9], single-arm plus an auxiliary suturing equipment based [10] [17], and dual-arm based systems have been successfully prototyped. Among them, dual-arm based implementations have been the mainstream in surgical knotting, which deal with the suture ends collaboratively for knot tying. In most cases, the dual-arm based robot has three translation degrees of freedom (DOFs) for each arm in order to move the suture ends in three dimensions [8]. For this reason, there has been standard protocol formalized for robotic knot tying [11]. Nowadays, pursuing less workspace consumption and minimally invasiveness has been the focus in robotic knot-tying research for better quality control and clinical compatibility [6]. With the dedicated efforts, currently available knot-tying robots usually work well on regular-size incision with 3-0 [14] or 2-0 [17] suture (U.S.P. standard). However, as the rapid development of microsurgery, there have been new challenges for robotic knot tying research, posed by tying micro-suture on mini-incision, like in vascular anastomosis [18]. Micro-suture has shorter and thinner geometry [19], leading to the difficulty of directly employing available knot-tying robots to meet the requirements in terms of spatial constraints, manipulating dexterity, higher precision, and better biomechanical compatibility [20].

In this work, we propose a dual-arm based nanorobot system for tying micro-suture on mini-incision under stereo microscope. Novelties and contributions are specified as:

1) A novel dual-arm based knot-tying nanorobot setup is proposed, featured by a rotation DOF mounted on each arm, endowing the system with additional manipulation dexterity.
2) A new motion trajectory planning is proposed for loop wrapping by synchronized coaxial rotation of the dual arms, which significantly reduces workspace consumption with shorter suture and increases mechanical compatibility to avoid tissue abrasion.
3) With the proposed system, we successfully realized tying two consecutive throws with opposition looping directions on 2.0 mm wide bionic blood vessel. The used micro-suture was 30 mm long #8-0 micro-suture.

Experimental results well validated the effectiveness of the proposed system: we achieved the smallest workspace consumption compared with state of the art. Meanwhile, the system also shows versatility of tying knots with 0, 1 and 2-0 suture, with all tied knots meeting the strengh requirements for clinical practice. The rest of this paper is organized as follows: Section II discusses the challenges facing tying micro-suture on mini-incision; Section III elaborates the nanorobot system; Section IV illustrates the experiments; Section V concludes this paper.

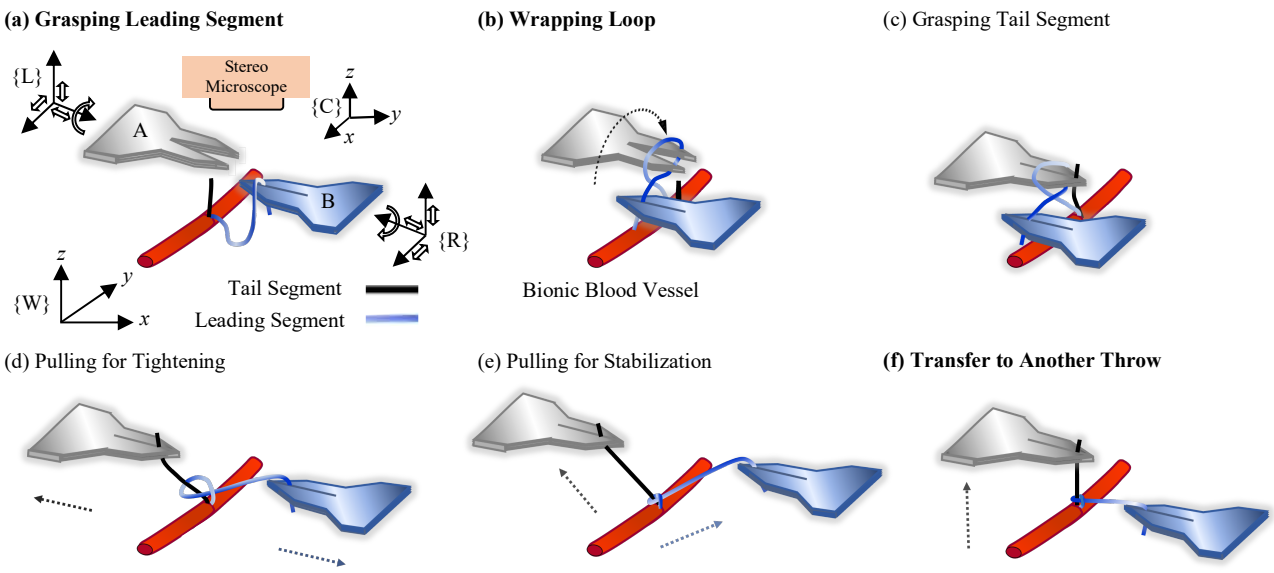

Fig. 1. Schematic pipeline illustrating the automated surgical knot tying with the coordinated nanorobotic manipulation. (a) conceptually shows the system setup proposed in this work. The gripper A and B are mounted with 3 translation degree of freedoms (DOFs) and one rotation DOF. The pipeline from (a) to (e) primarily follows the conventional knot tying process from literature, but with the loop-wrapping step (b) optimized by the rotation operation, leading to shorter motion path, smaller space consumption, and higher knotting efficiency. An additional step (f) is cascaded to this process in order to transfer the knot tying smoothly to next throw consecutively.

II. Overview of Nanorobot Knotting

A. General Steps of Automated Knot Tying

A surgical knot consists of two consecutive throws. The process to tie one throw is illustrated in Fig. 1. By convention, we define the longer segment of the suture thread as the leading segment, while the shorter segment as the tail segment. The two grippers of the dual-arm nanorobot are respectively defined as gripper A and gripper B. So procedurally, knot typing is described as: (a) gripper B holds the leading segment and wraps it around gripper A to form a loop, where A is in an open state and B is in a closed state; (b)-(c) gripper A goes through the loop to grasp the tail segment and pulls it backward through the loop; (d)-(e) both grippers simultaneously move towards opposite directions to tighten the thread. Up to now, the first throw is accomplished. Repeat (a)-(e) step with opposition looping direction in step (b) yields the second throw for a complete knot. Note that between two consecutive throws, a transitional step, as Fig. 1 (f), is designed where we control gripper A to ensure the tail segment remain upright before starting the second throw, which has not got enough attention in literature.

B. Research Problem Statement

This paper aims to solve the challenge of robotic knot tying on mini-incision, like in vascular anastomosis or other microsurgical procedure. As pointed in introduction, knot tying on mini-incision essentiates working in much limited space with shorter and thinner suture for less tissue abrasion. These requirements pose challenges to the implementation of knot-tying robot system in terms of dexterity, precision, as well as biomechanical compatibility. As the first effort in this regard, the specific challenges are discussed as follows.

First, shorter and thinner suture leads to more severe coupling effect [21], meaning that when manipulating one end of suture, the other end will undergo unexpected and uncertain motion more susceptibly; Second, shorter and thinner suture also results in the fact that the knot tying procedure, as shown by Fig. 1 (a)-(e), is supposed to be elaborately operated in much limited space; Third, micro-suture (30-50 μm in width) is more susceptible to microscale forces, particularly the capillary force in surgical wetting environment. Considering the super-flexibility, micro-suture will be more easily attached to tissue surface, making the grasping operation of suture end more difficult. Therefore, we must conduct more sophisticated motion trajectory planning and control for knot tying with micro-suture.

Nanorobotics provides a competent approach to overcome these aforementioned challenges for its high precision repeatability. To this end, we propose an efficient dual-arm nanorobotic system for automated knot tying on mini-incision with micro-suture, as illustrated by Fig. 1 (a), with each arm featured by 3 translation degree of freedoms (DOFs) and one rotation DOF. The additional rotation DOF endows the system with extra dexterity for tying knot in limited space. It is for sure that knot tying on mini-incisions presents other distinct challenges, including the crucial requirement for meticulous force regulation to prevent any mechanical abrasion to tissue. This aspect warrants dedicated and systematic research efforts in an in vivo setup. As an exploratory study, this work focuses on the kinematic motion planning of knot tying based on dual-arm nanorobot under the setting of bionic blood vessel for future endeavor. Thus, the task of knot tying on mini-incision in this work is specified as: based on the nanorobot as shown in Fig. 2, tie a surgical knot with two consecutive throws on 2.0 mm wide bionic blood vessel with 30 mm long #8-0 micro-suture.

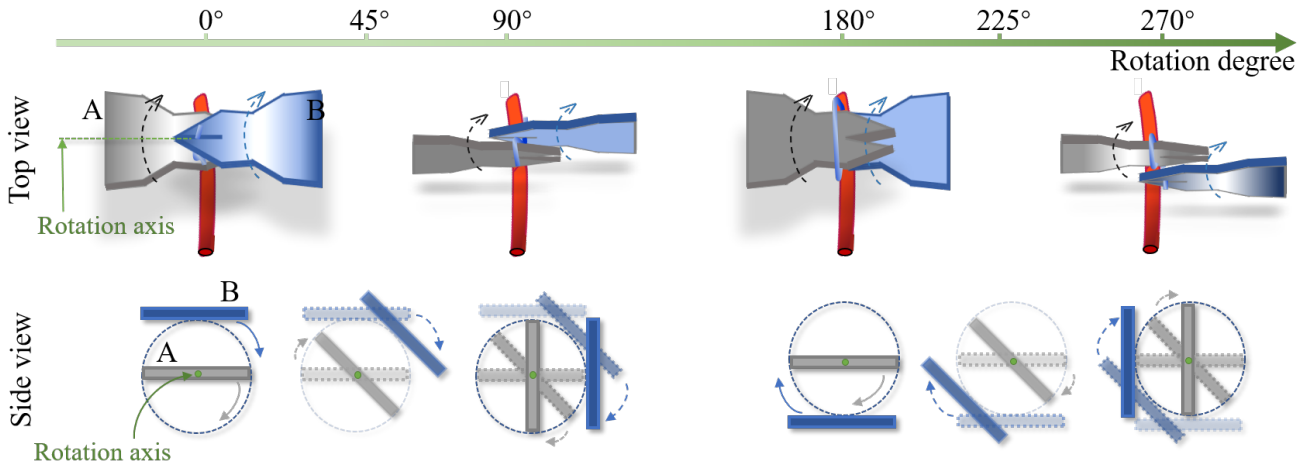

Fig. 3. Optimized trajectory planning for loop-wrapping by synchronized coaxial rotation of grippers to reduce workspace and suture length consumption.

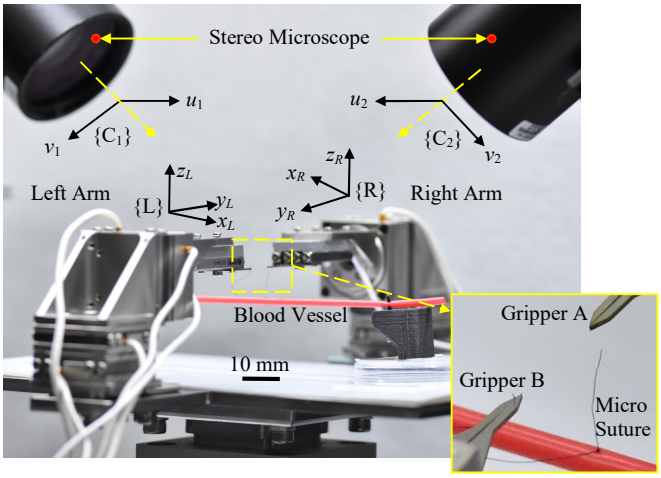

Fig. 2 The dual-arm knot-tying nanorobot system setup.

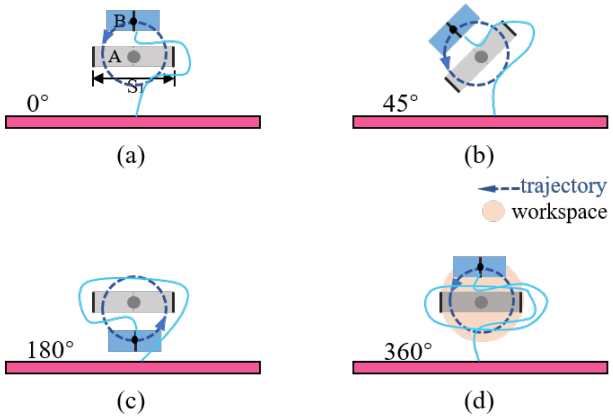

Fig. 4 Workspace consumption with the proposed loop-wrapping trajectory.

III. Methodology

A. Knot-Tying Nanorobot System Setup

The knot-tying system illustrated by Fig. 1 (a) is prototyped to conduct the study, primarily consisting of a dual-arm nanorobot, a binocular microscopic vision system, and a host computer, as depicted in Fig. 2. Two micro-grippers (SmarAct SG-1730 Micro-gripper, Gripping force is 1 N) are attached to left and right arm of the nanorobot. Each arm has three Attocube piezoelectric nanopositioner ECSx3030 (resolution is 1 nm, travel distance is 20 mm) as translation DOFs and one Attocube piezoelectric rotator ECR3030 as rotation DOF (resolution is 1 μ°, travel range is 360°). The stereo microscope has two Prosilica GC2450 cameras (resolution is 2448×2048, capturing 15 frames per second) mounted with telecentric lens (Coolens DTCM230-36). The host computer takes charge of the entire automated knot tying process. The knot tying task is tested on 2.0 mm wide bionic blood vessel. The coordinates are also given in Fig. 2, including image coordinates $\{C_1\}$ and $\{C_2\}$ and gripper coordinates {L} and {R} for left and right arm.

B. Trajectory Planning for Dual-Arm Knot Tying

The knot-tying procedure in this work also follows the conventional protocol illustrated by Fig. (a) to (e), but with the loop-wrapping step, i.e., Fig. 1 (b), optimized by the rotation DOF in order to meet the requirements of tying knots in much limited space with shorter and thinner suture. In specific, we propose a dynamic synchronized coaxial rotation motion trajectory as shown in Fig. 3.

Initially, gripper B holding the leading segment sits parallelly above gripper A. The y_L-axis serves as rotation axis, about which gripper A and B rotate simultaneously at the same angular velocity. Meanwhile, the distance between the two grippers is maintained constantly during the process to avoid unexpected collision within limited workspace. Accompanied with the rotation of gripper B, the suture forms a loop entangling around gripper A. Fig. 4 depicts the statuses of gripper A (gray) and gripper B (blue) in different rotation angles from both top view and side view for reader clarity. With 360°synchronized coaxial rotation, a suture loop is yielded and the grippers go back to the initial postures for the following steps.

For conventional loop-wrapping step, gripper B should keep as far as possible away from gripper A in order keep the leading segment in tension to avoid loop slipping from the gripper A, which substantially increases the workspace consumption and dragging force during loop wrapping. Fig. 3 conceptually shows the workspace spanned by the synchronized coaxial rotation of grippers with the proposed loop-wrapping motion trajectory. As can be seen from Fig. 3 that, unlike by conventional loop-wrapping motion strategy, no suture loop will be wrapped on gripper A, which further shortens the necessary suture length for loop wrapping.

The smooth transfer for two consecutive throws is also an important issue for knot tying with micro-suture to avoid being attached to tissue surface by capillary forces. In addition, to keep the tail segment in view for easy grasping during tying second throw, a new step is added to the standard knot tying protocol, given by Fig. 1 (f). Once the first throw is finished, gripper A moves upwards to pull the tail segment straight up in order to restore the initial state of knot tying given by Fig. 1 (a).

C. *Visual Servo based Control Scheme*

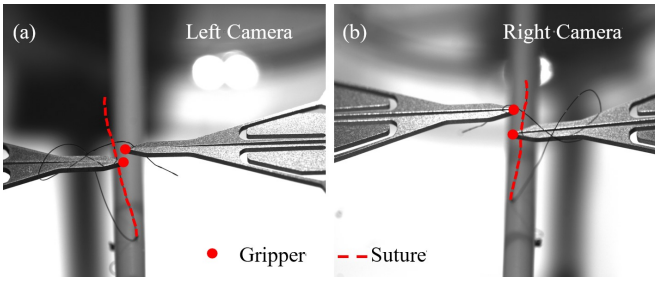

Fig. 5The features extracted from image for closed loop visual servo control.

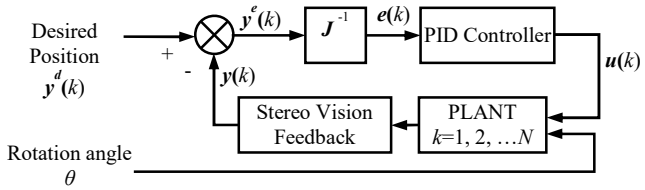

Fig. 6 The control block diagram for visual servo control during knot tying.

To precisely control the nanorobot to follow the designed motion trajectory, closed loop visual servo is included in the knot tying system. To this end, we need first to calibrate the image Jacobian matrix $\boldsymbol{J_L}$ and $\boldsymbol{J_R}$ of the nanorobot system, which establishes the hand-eye relationship for the left and right arm with respect to the stereo vision. With the image Jacobian matrix based visual servo control [23], the features extracted from images are given by Fig. 5, including the gripper tips and suture segments. When employing template matching, both grippers in two different views of camera are tracked to determine their position. The line segment feature is first tracked coarsely by applying Hough Transform to an edge image generated using Canny operator. The line segment feature is then finely reconstructed through connecting components in the edge image.

Fig. 6 presents the control block diagram for both arms for different steps of knot tying, where an integral controller is adopted as given by

$$\boldsymbol{u}(k) = K_I \cdot \boldsymbol{e}(k)\,. \tag{1}$$

The desired position $y^d(k)$ can be a fixed coordinate or coordinate sequence, depending on task specifications. The rotation angle θ is set zero unless in the case of loop wrapping. The stereo microscope extracts image features to get position misalignment error $y^e(k)$ in image space, which is further converted to position misalignment error $e(k)$ in Cartesian space by the pseudo inverse of the image Jacobian matrix. Note the $\boldsymbol{J_L}$ and $\boldsymbol{J_R}$ are 4×3 in dimension; the $y^d(k)$ is 4 × 1 vector; the $e(k)$ is 3 × 1 vector.

IV. Experiment and Results

To comprehensively evaluate the effectiveness of the proposed dual-arm nanorobot system setup given in Section III.A for automated knot tying on mini-incision with micro-suture, experiments were well conducted on 2.0 mm wide bionic blood vessel with 30 mm long #8-0 micro-suture to simulate the scenario of microvascular anastomosis microsurgery. We also carried out experiments to highlight the superiority of the proposed trajectory planning for loop wrapping in regard to decreasing workspace consumption. Finally, the tied knots were evaluated in terms of strength with different suture sizes to assess the proposed system for different potential medical applications.

A. *Automated Knot Tying with Two Consecutive Throws*

The proposed knot-tying system follows the standard knot-tying protocol, as illustrated by Fig. 1. The dual-arm based nanorobot system has one rotation DOF on each arm, enabling the synchronized coaxial rotation of grippers for loop wrapping in Fig. 1 (b), which is realized by the visual servo control given in Section III.C. Essentially, during synchronized coaxial rotation of grippers, one gripper goes through in-situ rotation, while the other gripper experiences off-axis rotation, both of which requires dedicated control. As demonstrated by Fig. 7 (a), the planned trajectory for gripper A is a fixed point, while it is a circle for gripper B. During experiments, the parameter θ was 5° in Fig. 6, and the integral coefficient K_I in Eq. (1) was 0.9. As can be seen, both grippers followed the planned trajectories quite well. Fig. 7 (b) shows the misalignment errors of the grippers along the planned trajectories, where the average error was about 0.8 mm. Fig. 7 (c) shows the entire motion trajectories of both grippers in 3D space during tying one throw. The entire workspace was extended by the pulling process, which can be further optimized by repetitive grasping and pulling of leading segment. The image Jacobian matrix (pixel/μm in unit) were calibrated as follows.

$$\boldsymbol{J_L} = \begin{bmatrix} 0.0004 & -0.0919 & -0.0061 \\ 0.0602 & -0.0042 & 0.0706 \\ 0.0013 & 0.0915 & 0.0007 \\ -0.0575 & 0.0003 & 0.0720 \end{bmatrix}, \boldsymbol{J_R} = \begin{bmatrix} -0.0594 & 0.0055 & 0.0707 \\ -0.0004 & 0.0921 & -0.0068 \\ -0.0023 & -0.0910 & 0.0012 \\ 0.0576 & 0.0008 & 0.0717 \end{bmatrix} \tag{2}$$

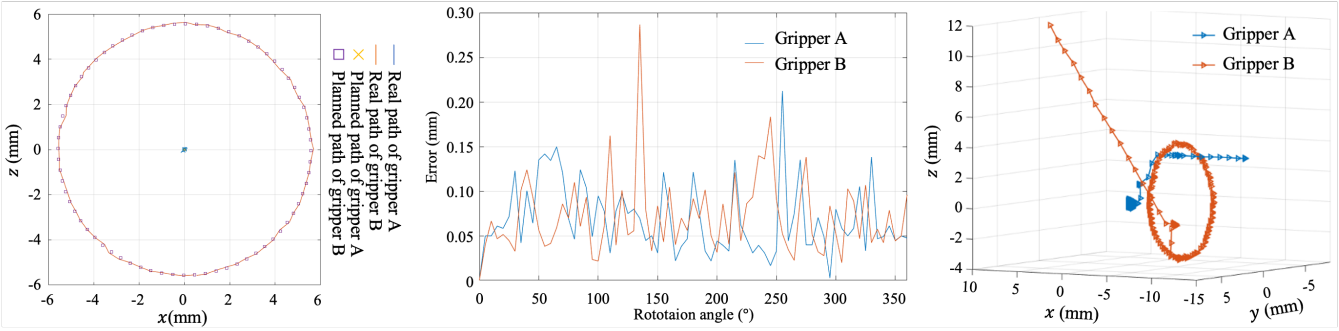

(a) (b) (c)

Fig. 7 Experiment results in tying one throw. (a) the planned and real trajectories during loop wrapping in XZ plane; (b) the misalignment error of both grippers during synchronized coaxial rotation; and (c) the motion trajectories of both grippers in 3D space during knot tying.

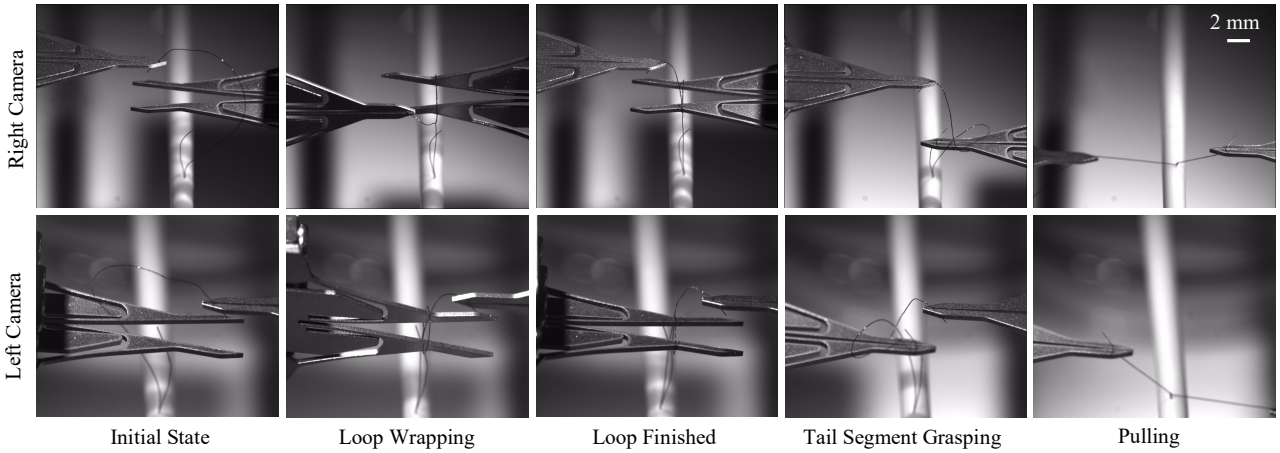

Fig. 8 The sequential images captured from stereo microscope during the knot-tying process.

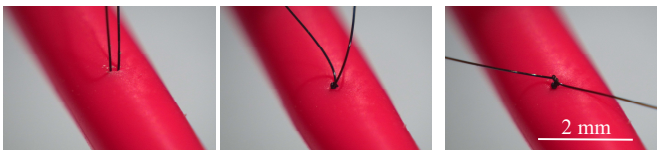

Fig. 9 The tied knot with two consecutive throws.

Fig. 8 shows the sequential images captured by the stereo microscope at different steps during the knot-tying process. During the entire process, both grippers were well controlled within the field of view of microscope. Meanwhile, both grippers were controlled within the depth of field avoiding the image blurring problem. On average, it took about 3 mins to tie one throw. Finally, since the loop-wrapping is realized by synchronized coaxial rotation of grippers, unlike by maintaining a fixed dragging force along the leading segment in traditional approach, we barely experienced no loop slipping from the gripper, thus guaranteed the operation successes rate to 100%. Fig. 9 shows the tied knot captured by a recording camera, corresponding to the initial state, the first throw, and the second throw on bionic blood vessel.

B. Workspace Consumption and Knot Strength

To highlight the advantage of the proposed trajectory planning for loop wrapping in terms of reducing workspace consumption, we used the nanorobot to perform loop wrapping operation with three other existing state-of-the-art methods, including the traditional method [23], the "rolling arc looping" proposed by Chow *et al.* [8] (motion trajectories of grippers were generated with 30 mm long suture, shown by Fig. 10 (a)), and that proposed by Lu *et al.* [6] (motion trajectories of grippers were generated with 50 mm long suture, shown by Fig. 10 (b)). Fig. 10 (c) demonstrates the workspace consumption (in terms of spanning area in XZ plane) of the four different methods against different suture lengths. As can be seen, for the compared loop-wrapping methods, workspace consumption increases along with longer suture length, while the workspace consumption keeps constant regardless of the suture length for the proposed motion trajectory planning. Most importantly, benefited from the synchronized coaxial rotation of grippers for loop wrapping, the proposed trajectory planning consumed the least workspace for all circumstances, which conforms our claimed contribution.

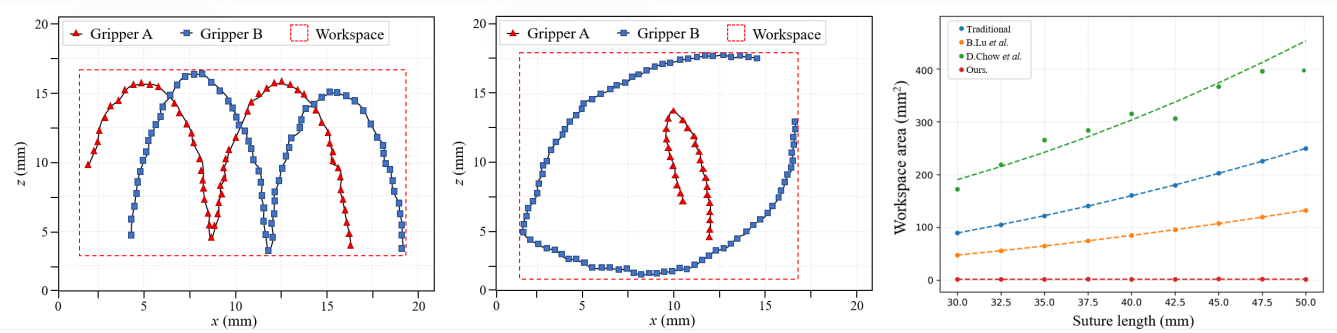

(a) (b) (c)

Fig. 10. Comparison experiments of workspace consumption for loop wrapping performed on our nanorobot. (a) The motion trajectories of grippers were generated with 30 mm long suture by Chow *et al.*; (b) The motion trajectories of grippers were generated with 50 mm long suture by Lu *et al.* method; (c) The workspace consumption of different methods against suture length.

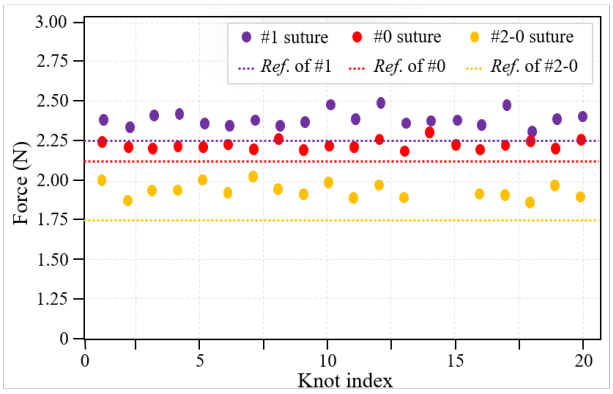

Fig. 11 The evaluated knot strength in terms of sliding friction force with different suture types.

Knot quality is critical for surgery success and postoperative recovery to avoid surgery complex or infection. To this end, we also tested the knot quality in terms of knot strength by sliding friction force with the method in [4] to evaluate the effectiveness of proposed knot-tying nanorobot system in clinical applications. In specific, the knot strength was evaluated by measuring knot slipping friction force with distinct types of sutures, including #1 suture (diameter is 0.4 mm - 0.499 mm), #0 suture (diameter is 0.35 mm - 0.399 mm), and #2-0 suture (diameter is 0.3 mm -0.349 mm) suture. The referred knot strength for quality comparison baseline was obtained by measuring and analyzing the surgical knots tied by experienced surgeons. As illustrated by Fig. 10, with the proposed dual-arm based nanorobot system, the tied knots showed up adequate and stronger strength for different suture types compared with reference values, thus met clinical requirements for potential medical scenarios. Meanwhile, with various suture types, knot strength manifested good consistency, thus highlighting the repetitiveness and reliability of the proposed knot-tying system in practical applications. Meanwhile, we injected water constantly into the sutured bionic blood vessel at 120mmHg pressure for 1 min and witnessed no leakage, which also served as evidence of reliability of the system.

V. Conclusion

In this paper, we proposed a novel dual-arm based nanorobot system for automated knot tying performed on mini-incision under stereo microscope, featured by an additional rotation DOF on each arm. With this setup, an optimized motion trajectory planning by synchronized coaxial rotation of grippers is also presented in order to support tying knots with shorter and thinner suture. Leveraging the natural advantage of nanorobotics and microscope, the proposed system is capable of tying consecutive throws with micro-suture on mini-incision, like in vascular anastomosis or microsurgery. We successfully evaluated the knot tying system on 2.0 mm wide bionic blood vessel with 30 mm long #8-0 micro-suture. Experiment results also validated that: the proposed nanorobot system can realize reliable knot tying within smallest workspace compared with state-of-the-art methods; the tied knots exhibit adequate knot strength, meeting the requirements of clinical applications.

The authors are well aware of the fact that knot tying is a complicated process, which should not be isolated from the background surgery for separated research. Therefore, there is definitely space for the proposed knot-tying nanorobot system to further improve its performance, particularly to incorporate force sensor into the system to increase its mechanical compatibility to avoid tissue abrasion. However, this work focuses on the kinematic motion planning of knot tying based on dual-arm nanorobot under the setting of bionic blood vessel as an exploratory study. In our future endeavor, we will apply the proposed knot-tying system to practical vascular anastomosis *in vivo*.

References

[1] P. Sundaresan, J. Grannen, B. Thananjeyan, A. Balakrishna, M. Laskey, K. Stone, and J. E. Gonzalez, and K. Goldberg, "Learning Rope Manipulation Policies Using Dense Object Descriptors Trained on Synthetic Depth Data," *IEEE International Conference on Robotics and Automation*, Paris, France, 2020, pp. 9411-9418.

[2] W. Wang and D. Balkcom, "Tying Knot Precisely," *IEEE International Conference on Robotics and Automation*, Stockholm,

Sweden, 2016, pp. 3639-3646.

[3] D. L. Chow, R. C. Jackson, M. C. Çavuşoğlu, and W. Newman, "A Novel Vision Guided Knot-tying Method for Autonomous Robotic Surgery," *IEEE International Conference on Automation Science and Engineering*, New Taipei, Taiwan, 2014, pp. 504-508.

[4] P. Johanns, C. Baek, P. Grandgeorge, S. Guerid, S. A. Chester, and P. M. Reis, "The Strength of Surgical Knots Involves a Critical Interplay Between Friction and Elastoplasticity," Science Advances, vol. 9, no. 23, pp. eadg8861, 2023.

[5] R. Singh and W. Hawkins, "Sutures, Ligatures and Knots," Surgery (Oxford), vol. 38, no. 3, pp. 123-127, 2020.

[6] B. Lu, H. K. Chu, K. C. Huang, and L. Cheng, "Vision-Based Surgical Suture Looping Through Trajectory Planning for Wound Suturing," *IEEE Transactions on Automation Science and Engineering*, vol. 16, no. 2, pp. 542-556, 2019.

[7] T. Osa, N. Sugita, and M. Mitsuishi, "Online Trajectory Planning and Force Control for Automation of Surgical Tasks," *IEEE Transactions on Automation Science and Engineering*, vol. 15, no. 2, pp. 675-691, 2018.

[8] D. L. Chow and W. Newman, "Improved Knot-tying Methods for Autonomous Robot Surgery," *IEEE International Conference on Automation Science and Engineering*, Madison, WI, USA, 2013, pp. 461-465.

[9] S. A. Pedram, C. Shin, P. W. Ferguson, J. Ma, E. P. Dutson, and J. Rosen, "Autonomous Suturing Framework and Quantification Using a Cable-Driven Surgical Robot," *IEEE Transactions on Robotics*, vol. 37, no. 2, pp. 404-417, 2021.

[10] S. Leonard, A. Shademan, Y. Kim, A. Krieger, and P. C. W. Kim, "Smart Tissue Anastomosis Robot (STAR): Accuracy evaluation for supervisory suturing using near-infrared fluorescent markers," *IEEE International Conference on Robotics and Automation*, Hong Kong, China, 2014, pp. 1889-1894.

[11] S. A. Pedram, P. Ferguson, J. Ma, E. Dutson, and J. Rosen, "Autonomous suturing via surgical robot: An algorithm for optimal selection of needle diameter, shape, and path," *IEEE International Conference on Robotics and Automation*, Singapore, 2017, pp. 2391-2398.

[12] F. Zhong, Y. Wang, Z. Wang, and Y. H. Liu, "Dual-Arm Robotic Needle Insertion with Active Tissue Deformation for Autonomous Suturing," *IEEE Robotics and Automation Letters*, vol. 4, no. 3, pp. 2669-2676, 2019.

[13] G. B. Cadière, J. Himpens, M. Poras, L. Pau, N. Boyer, and B. Cadiere, "First Human Surgery Using a Surgical Assistance Robotics Device for Laparoscopic Cholecystectomies," Surgical Endoscopy, pp. 1-7, 2023

[14] L. Cao, X. Li, P. T. Phan, A. M. Tiong, H. L. Kann, J. Liu, W. Lai, Y. Huang, H. M. Le, M. Miyasaka, and K. Y. Ho, "Sewing Up the Wounds: A Robotic Suturing System for Flexible Endoscopy," IEEE *Robotics & Automation Magazine*, vol. 27, no. 3, pp. 45-54, 2020.

[15] B. Lu, H. K. Chu, and L. Cheng, "Dynamic trajectory planning for robotic knot tying," *IEEE International Conference on Real-time Computing and Robotics*, Angkor Wat, Cambodia, 2016, pp. 180-185.

[16] Y. Hu, W. Li, L. Zhang, and G. Z. Yang, "Designing, Prototyping, and Testing a Flexible Suturing Robot for Transanal Endoscopic Microsurgery," *IEEE Robotics and Automation Letters*, vol. 4, no. 2, pp. 1669-1675, 2019.

[17] H. Saeidi, H. N. D. Le, J. D. Opfermann, S. Leonard, A. Kim, M. H. Heieh, J. U. Kang, and A. Krieger, "Autonomous Laparoscopic Robotic Suturing with a Novel Actuated Suturing Tool and 3D Endoscope," *International Conference on Robotics and Automation*, Montreal, QC, Canada, 2019, pp. 1541-1547.

[18] G. Malzone, G. Menichini, M. Innocenti, and A. Ballestin, "Microsurgical Robotic System Enables the Performance of Microvascular Anastomoses: a Randomized in vivo Preclinical trial," *Scientific Reports*, vol. 13, no. 1, pp. 14003, 2023.

[19] M. H. Korayem and V. Vahidifar, "Detecting Hand's Tremor Using Leap Motion Controller in Guiding Surgical Robot Arms and Laparoscopic Scissors", *Measurement*, vol 204, pp.112133, 2022.

[20] T. J. Mulken, R. M. Schols, A. M. Scharmga, B. Winkens, R. Cau, F. B. Schoenmakers, S. S. Qiu, and R. R. Hulst, "First-in-human Robotic Supermicrosurgery Using a Dedicated Microsurgical Robot for Treating Breast Cancer-related Lymphedema: a Randomized Pilot Trial," *Nature Communications*, vol. 11, no. 1, pp. 757, 2020.

[21] B. Kubiak, N. Pietroni, F. Ganovelli, and M. Fratarcangeli, "A Robust Method for Real-time Thread Simulation," *ACM symposium on Virtual Reality Software and Technology, Association for Computing Machinery*, New York, 2007.

[22] S. Liu, D. Xu, D. Zhang, and Z. Zhang, "High Precision Automatic Assembly Based on Microscopic Vision and Force Information," *IEEE Transactions on Automation Science and Engineering*, vol. 13, no. 1, pp. 382–393, 2016.

[23] H. Kang and J. T. Wen, "Autonomous Suturing Using Minimally Invasive Surgical Robots," *IEEE International Conference on Control Applications*, Anchorage, AK, USA, 2000, pp. 742-747.